Photonic defect modes in a cholesteric liquid crystal with a resonant nanocomposite layer and a twist defect

Stepan Ya. Vetrov,[1,2] Maxim V. Pyatnov,[1,2,3,*] and Ivan V. Timofeev[1,4]

[1]*L.V. Kirensky Institute of Physics, Siberian Branch of the Russian Academy of Sciences, Krasnoyarsk 660036, Russia*

[2]*Institute of Engineering Physics and Radio Electronics, Siberian Federal University, Krasnoyarsk 660041, Russia*

[3]*Krasnoyarsk State Medical University named after Professor V.F. Voyno-Yasenetsky, Krasnoyarsk 660022, Russia*

[4]*Laboratory for Nonlinear Optics and Spectroscopy, Siberian Federal University, Krasnoyarsk 660041, Russia*

(Received 26 June 2014; published 24 September 2014)

We have studied spectral properties of a cholesteric liquid crystal with a combined defect consisting of a nanocomposite layer and a twist. The nanocomposite layer is made of metallic nanoballs dispersed in a transparent matrix and featuring effective resonant permittivity. A solution has been found for the transmission spectrum of circularly polarized waves in the structure. We have analyzed spectral splitting of the defect mode in the band gap of the cholesteric when its frequency coincides with the nanocomposite resonant frequency. Defect modes have characteristics strongly dependent on the magnitude and the sign of the phase difference of the cholesteric helix on both sides of the defect layer. It has been found that the band gap width and the position and localization degree of defect modes can be effectively controlled by external fields applied to the cholesteric.

DOI: 10.1103/PhysRevE.90.032505 PACS number(s): 42.70.Df, 61.30.Gd, 42.70.Qs, 78.67.Sc

I. INTRODUCTION

Photonic crystals (PCs) attract much interest due to their special optical properties and versatile application potential [1–4]. Such materials are unique in that their dielectric permittivity can change periodically in one, two, or three dimensions at a spatial scale comparable with the light wavelength. There is a fairly close formal analogy between the theory of propagation of electromagnetic waves in periodic media and the quantum theory of electrons in crystals. The zone structure of the electron energy spectrum associated with the Bragg reflection of electrons is similar to that of a PC. In photonic band gaps (PBGs) of PCs with a lattice defect, i.e., with a disturbed periodicity, there emerge transmission bands with the location and transmission coefficient controllable by geometrical and structural parameters. Note that light is localized in the defect area, which enhances the light wave intensity inside the defect layer.

Cholesteric liquid crystals (CLCs) belong to a special class of one-dimensional PCs possessing unique properties, namely, broad transparency band, strong nonlinearity, and high susceptibility to external low-frequency electric or magnetic fields as well as to applied light or heat [5,6]. The CLC helix pitch and location of the band gap can be essentially changed by varying temperature and pressure and applying electromagnetic fields or mechanical stress. The qualitative difference of CLCs from any other type of PC lies in their polarization selectivity by diffractive reflection. In CLCs there are PBGs for light propagating along the CLC helix with a circular polarization coinciding with the twist of the CLC helix. When reflected from the CLC, a light wave of such polarization does not change the sign of its polarization.

Bragg reflection occurs in the wavelength range between $\lambda_1 = pn_o$ and $\lambda_2 = pn_e$, where p is the helix pitch and n_o and n_e are the ordinary and extraordinary refractive indices of the CLC. Light of opposite circular polarization does not undergo diffractive reflection and passes through a CLC medium almost unaffected.

Introducing various types of defects into the structure of an ideal cholesteric makes it possible to obtain narrow transmission bands in PC band gaps that will correspond to localized defect modes. These modes, similar to defect modes in scalar periodic layered media, can be used to produce narrow band and tunable filters [7], optical diodes [8], a liquid crystal rotator and a tunable polarizer [9], polarization azimuth rotation and azimuth stabilizers [10], and other devices. Low threshold laser generation in the CLC is under extensive research [11]. There are two possible options for such generation: band edge lasing [12] and defect mode lasing [13].

There exist a few ways of inducing photonic defect modes in the CLC. This can be achieved by using a thin layer of an isotropic [14] or anisotropic substance [13,15] confined between two layers of the CLC, twist defect (jump of the rotation angle of the cholesteric helix), [16–18] or defect associated with local changes in the helix pitch [19–21]. The authors of Ref. [22], using an analytical approach to the theory of optical defect modes in a CLC with an isotropic defect layer, developed a model that isolates polarization mixing and yields a light equation only for diffractive polarization. Analysis of defect modes in the CLC induced by twist defect, i.e., by a sharp turn of the director around the CLC axis at the interface of two CLC layers, can be found in Refs. [23,24]. The direction of predominant orientation of molecules in the CLC is referred to as a CLC director. Propagation of light in a CLC containing a dielectric layer combined with a twist defect at the interface between the dielectric and the CLC layer was studied in Refs. [7,25]. PCs doped with substances having strong optical resonance are under extensive research. An example of a giant optical resonance has been predicted for a nanocomposite (NC) consisting of metallic nanoballs dispersed in a transparent matrix [26], whereas the optical characteristics of primary materials lack resonant properties. The resonance is characterized by effective permittivity in approximation of the Maxwell Garnett formula, which is proved by both the numerical simulation [27] and the experiment [28].

*Corresponding author: MaksPyatnov@yandex.ru

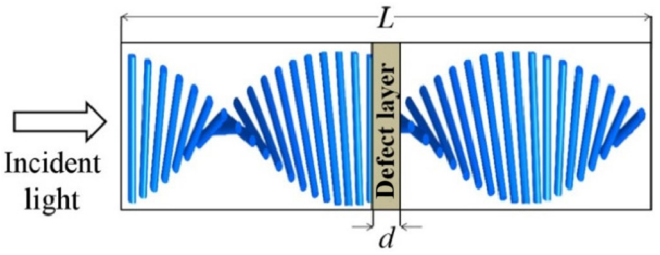

FIG. 1. (Color online) Schematic of the CLC with a combination of defects.

The effective characteristics of a NC containing metallic nanoparticles dispersed in a dielectric matrix are due to the plasmon resonance of nanoparticles. These characteristics can have unique magnitudes not inherent in natural materials. For instance, the effective refractive index can be in excess of 10. Dispersion of resonant medium combined with the PC dispersion provides a new tool to control spectral and optical properties of PCs [29–31].

Our study is focused on spectral properties of a CLC with a combined defect. A NC layer with resonant dispersion and a cholesteric helix phase jump at the interface of the nanocomposite layer, and cholesteric layers serve as such a defect. Splitting of the defect mode and localization of the electromagnetic field are analyzed depending on the volume fraction of nanoparticles in the defect layer. Phase jump of the CLC helix in the transmission spectrum is discussed. We also study modification of the transmission spectrum of the cholesteric with a combined defect under external fields affecting the CLC helix pitch.

II. MODEL AND TRANSMITTANCE

The PC structure under consideration consists of two identical layers of a CLC with a right-handed twist separated by a NC defect layer combined with a twist defect (Fig. 1). The length of the entire structure is $L = 2.946\ \mu$m, the CLC helix pitch is $p = 275$ nm, and the defect layer thickness is $d = 196$ nm. The medium outside the CLC is isotropic and has the refractive index $n = (n_o + n_e)/2$, where $n_o = 1.4$ and $n_e = 1.6$ are the ordinary and extraordinary refractive indices, respectively, of the cholesteric. For the chosen external medium, Fresnel reflection from the CLC surface and interference processes from the boundary surfaces will be weak. The twist defect magnitude is governed by the angle α that is positive when the vector tip of the CLC director rotates clockwise at the interface between NC and CLC layers (conventionally observed along the direction of light propagation).

The effective permittivity of a NC layer $\varepsilon_{\rm mix}$ is found from the Maxwell Garnett formula widely used when dealing with matrix media where a small volume fraction of isolated inclusions is dispersed in the material matrix [26,32],

$$\varepsilon_{\rm mix} = \varepsilon_d\left[\frac{f}{(1-f)/3 + \varepsilon_d/(\varepsilon_m - \varepsilon_d)} + 1\right]. \qquad (1)$$

Here f is the filling factor, i.e., the fraction of nanoparticles in the matrix, ε_d and $\varepsilon_m(\omega)$ are the permittivities of the matrix and the metal of the nanoparticles, respectively, ω is the radiation frequency. The Maxwell Garnett model assumes quasistatic approximation. Metallic inclusions in the dielectric matrix are separated by distances much longer than their characteristic size. The characteristic size of inclusions is small compared to the wavelength of light in an efficient environment. To find the permittivity of the metal of the nanoparticles using the Drude approximation,

$$\varepsilon_m(\omega) = \varepsilon_0 - \frac{\omega_p^2}{\omega(\omega + i\gamma)}, \qquad (2)$$

where ε_0 is the background dielectric constant taking into account contributions from interband transitions, ω_p is the plasma frequency, and γ is the plasma relaxation rate. For silver nanoballs dispersed in a transparent optical glass, $\varepsilon_0 = 5$, $\hbar\omega_p = 9$ eV, $\hbar\gamma = 0.02$ eV, and $\varepsilon_d = 2.56$. Thus, in this paper calculations are carried out without taking into account the correction of the dielectric function of metal nanoparticles taking into account the limitation of the electron mean free path due to its collision with the boundary of the particle. The model predictions of the Maxwell Garnett effective medium are valid for moderate proportion of inclusions with a filling factor of $f \ll 1$ [27].

Ignoring the small factor γ^2, we find the position of the resonant frequency that depends on the characteristics of

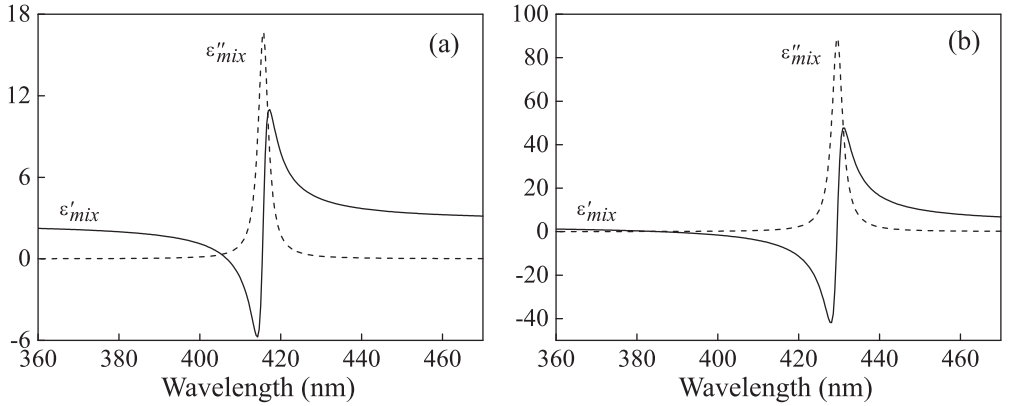

FIG. 2. Imaginary $\varepsilon''_{\rm mix}$ (dashed curve) and real $\varepsilon'_{\rm mix}$ (solid curve) parts of the effective permittivity $\varepsilon_{\rm mix}$ versus wavelength. The filling factors (a) $f = 0.02$ and (b) $f = 0.1$.

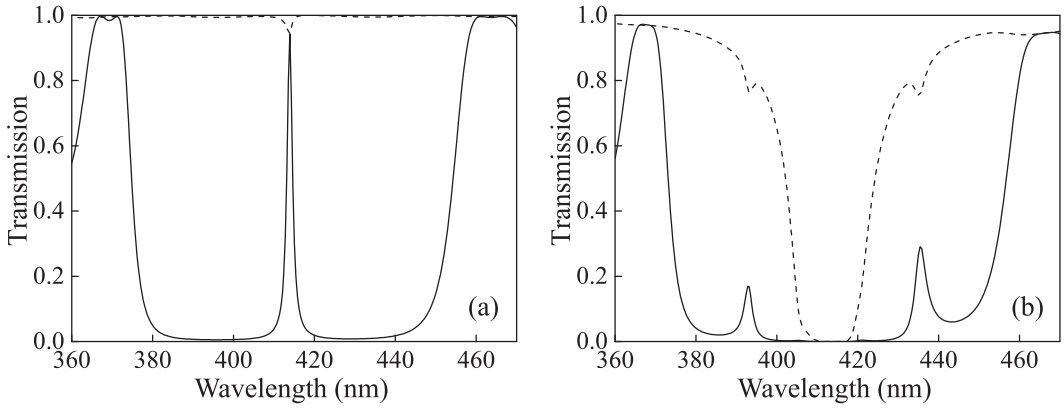

FIG. 3. Transmission spectrum for right- (solid curve) and left-handed (dashed curve) polarizations for $\alpha = 0$: (a) $f = 0$ and (b) $f = 0.02$.

primary materials and the dispersed phase concentration f:

$$\omega_0 = \omega_p \sqrt{\frac{1-f}{3\varepsilon_d + (1-f)(\varepsilon_0 - \varepsilon_d)}}. \tag{3}$$

Figure 2 shows dispersion dependence of the nanocomposite permittivity for two different filling factors: $f = 0.02, 0.1$. As can be seen in the figure, the ω_0 frequency corresponding to resonance in the defect layer shifts towards the long-wavelength range of the spectrum with the growing concentration of nanoballs. Note that the resonant curve half-width $\varepsilon''_{\text{mix}}$ is affected very little, whereas the $\varepsilon'_{\text{mix}}$ curve is essentially modified and the range of frequencies increases for which the NC is similar to metal when $\varepsilon'_{\text{mix}} < 0$. We employed the Berreman transfer matrix method for numerical analysis of the spectral properties and field distribution in the sample [33,34]. This provided us with a tool to numerically assess propagation of light in the cholesteric with a structural defect. An equation to describe light propagation at frequency ω along the z axis is given by

$$\frac{d\Psi}{dz} = \frac{i\omega}{c}\Delta(z)\Psi(z), \tag{4}$$

where $\Psi(z) = (E_x, H_y, E_y, -H_x)^T$ and $\Delta(z)$ is the Berreman matrix dependent on the permeability tensor and incident wave vector.

The proposed system can be fabricated according to the procedure described in Ref. [35]. Difficulty may be due to the small thickness of the nanocomposite layer. When assembling the cell the nanocomposite layer is in contact with the oriented CLC layers. A noncontact method is preferred for orientant applying. Wide annular spacers are required to ensure the flatness of a thin layer of the nanocomposite. Manipulation of the CLC optical characteristics by means of electrical, magnetic, optical fields, or temperature is a well known and robust technique.

III. RESULTS AND DISCUSSION

A. Optics of the CLC with a combined defect

Figure 3(a) shows a seed ($f = 0$) transmission spectrum for normal incidence of light on the CLC with a structural defect in the form of a dielectric platelet without a twist defect ($\alpha = 0$). One can see that similar to Ref. [14], there are peaks in the CLC PBG associated with CLC defect modes induced for normally incident light. Moreover, defect modes are associated with the same wavelength and the same transmission at the defect mode wavelength.

In Ref. [31] it was found that, similar to frequency splitting of two coupled oscillators, the defect mode frequency splits if the filling factor is nonzero and the NC resonant frequency ω_0 is close to the defect mode frequency. The effect of splitting

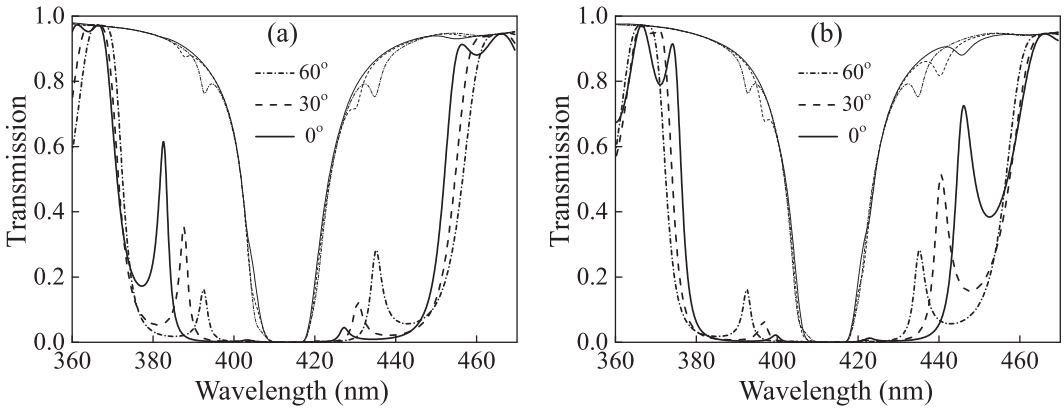

FIG. 4. Transmission spectra of the structure for various α's: (a) $\alpha > 0$ and (b) $\alpha < 0$. The bold curves refer to the right-handed circular polarizations, and the thin curves refer to the left-handed circular polarizations of light, $f = 0.02$.

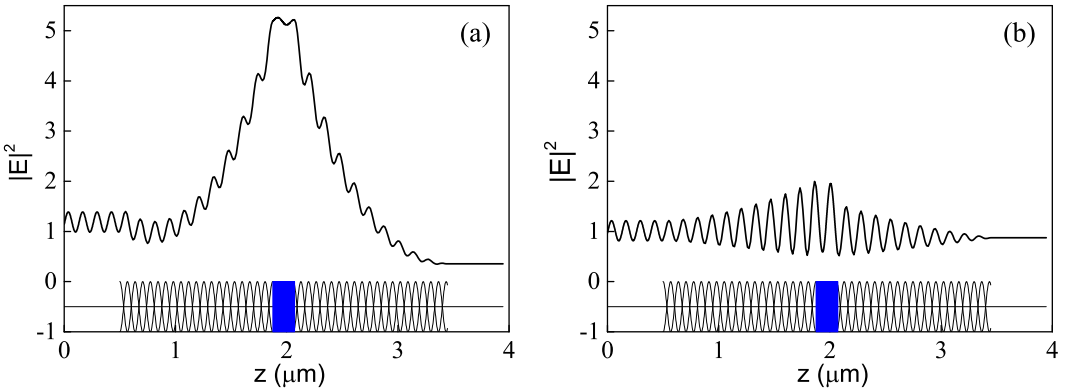

FIG. 5. (Color online) Distribution of the squared electric field modulus in defect modes with $\lambda = 388$ nm [option $\alpha = 30^\circ$ corresponds to option 2 in Fig. 4(a)]. (a) Wave with right-handed circular polarization and (b) wave with left-handed circular polarization, $f = 0.02$.

in the transmission spectrum is illustrated in Fig. 3(b). As can be seen in the figure, the resultant peaks have the same wavelength for the right- and left-handed polarizations but differ in transmittance in the peak center. Calculations show that the splitting enhances with the growing volume fraction of nanoballs in the composite as it happens in the case of a scalar one-dimensional PC with a resonant defect nanocomposite layer [29]. The reflection index and the absorption coefficient were found to be strongly dependent on the direction of circular polarization of incident light. The emergent band gap in the spectrum for both polarizations is primarily due to substantial reflection and absorption of waves with right-handed and left-handed polarizations, respectively.

The result of the twist defect is the repositioning of defect modes in the band gap of the CLC, which affects transmission at the defect mode frequency. Figure 4(a) shows that clockwise rotation of the second CLC layer ($\alpha > 0$) makes both peaks for right-handed and left-handed polarizations of light shift to the shorter-wavelength range. Transmittance of the long-wavelength peak drops down with the growing α, whereas that of the short-wavelength peak enhances. A reverse situation is observed when the CLC layer is rotated counterclockwise ($\alpha < 0$) [Fig. 4(b)]. Redistribution of transmission intensity at defect modes depending on α is obviously associated with their coupling due to the twist defect. No peaks of either polarization of light emerge in the band gap zone of the CLC for the chosen parameters of the system and $\alpha = 90^\circ$. Our calculations show that peaks for light of nondiffractive polarization are not observed just for any α. The band gap location is almost independent of the twist defect magnitude.

Figure 5 is an example of spatial distribution of an electric field in $\lambda = 388$ nm defect modes for $\alpha = 30^\circ$ [see Fig. 4(a)]. Field localization is most prominent in the area comparable with the wavelength for the peak corresponding to diffractive polarization.

Note that the number of cholesteric periods increases the steepness of the photonic band gap. Moreover, transmission peaks for the right diffracting and left circular polarization of light decrease for the defect having filling factor $f = 0$ [7]. Similar behavior of the defect modes peaks, with the number of periods of the cholesteric, also found in our case, when the filling factor of the nanocomposite metal particles is not zero. For example, for $f = 0.02$, $\alpha = 0$ [Fig. 3(b)], and 30 periods of each CLC helix, the total thickness of the structure being 16.696 μm, transmission peaks for the right circular polarization are already virtually indistinguishable from zero. However, the peaks transmission coefficients to the left polarization of light are 0.68 and 0.67, respectively.

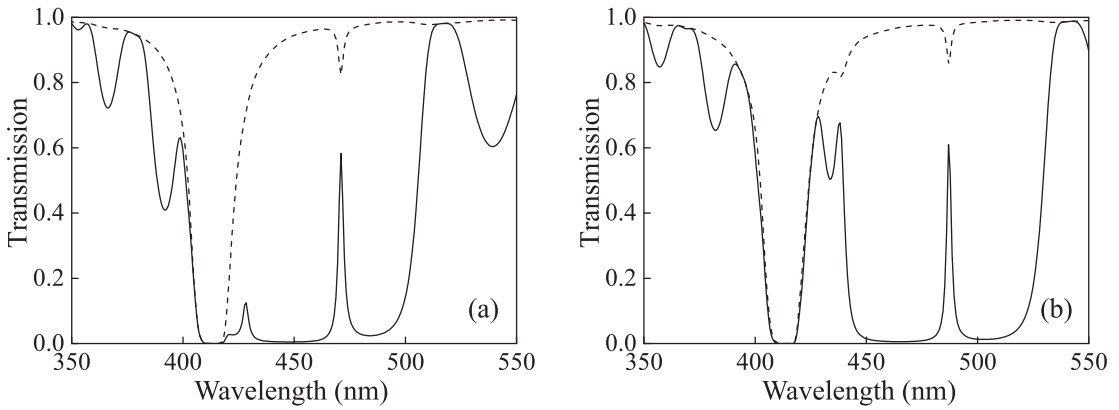

FIG. 6. Transmission spectrum for various helix pitches. (a) $p = 305$ nm and (b) $p = 320$ nm. The solid and dashed curves refer to the right-handed and left-handed circular polarizations of light, respectively, $f = 0.02$ and $\alpha = -30^\circ$.

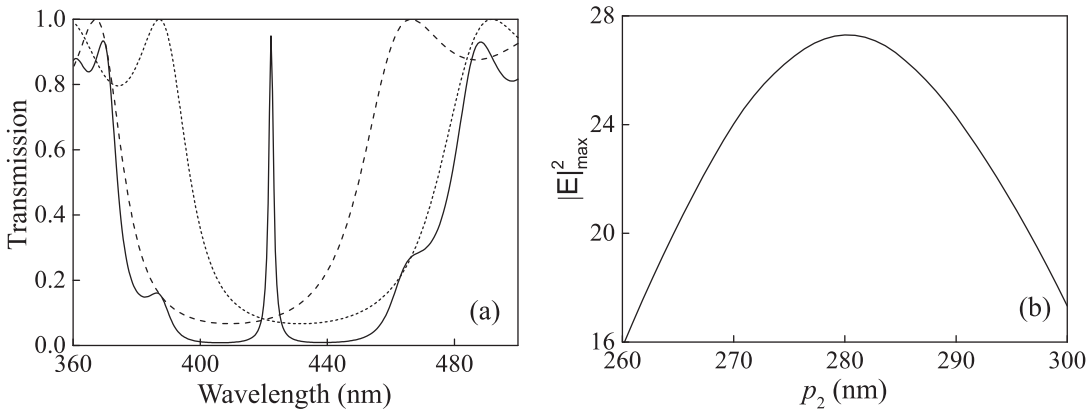

FIG. 7. (a) Transmission coefficient for a system of two cholesterics with a defect (solid curve) and for each of the cholesterics (dashed curve) with the pitch on the left of the defect $p_1 = 275$ nm (dotted curve) and $p_2 = 290$ nm (dotted curve). (b) Maximum squared modulus of the electric field of the defect mode as a function of the pitch p_2. The remaining parameters are the same as in Fig. 3(a).

B. Means to control the transmission spectrum of the CLC with a combined defect

By varying the CLC helix pitch p and the angle of light incidence on the sample it is possible to control the transmission spectrum behavior. Increasing the helix pitch, for example, by varying the temperature, results in a band gap shift to the long-wavelength region following the Bragg condition $pn = \lambda$. The short-wavelength peak corresponding to the defect mode disappears; the long-wavelength peak for the right- and left-handed circular polarizations of light remains. It is essential that there are pitches for which the resonance frequency ω_0 appears to be located close to the short-wavelength boundary of the PBG.

An example of the resultant changes in the transmission spectrum of the structure at $\alpha = -30°$ is illustrated in Fig. 6(a). The CLC helix pitch was changed from $p = 275$ nm to $p = 305$ nm, which made the NC resonant frequency ω_0 move close to the short-wavelength boundary of the PBG.

Band gap splitting is observed when the resonance mode is coupled with photonic modes. An extra transparency band induced by diffractive polarization splits off the short-wavelength edge to give rise to a band gap in the vicinity of ω_0 for light of both polarizations. The stop band is primarily the result of field absorption in the NC layer. A further increase in the helix pitch forces the resonant frequency ω_0 to shift to the continuous transmission spectrum. The developed resonance situation in this case facilitates the formation of an extra band gap in the transmission spectrum [Fig. 6(b)].

An alternative approach to realize similar effects is to increase the angle of light incidence on the structure. Then, following the Bragg condition, the band gap will shift toward the short-wavelength range while the long-wavelength edge of PBG comes closer to the resonant frequency ω_0 of the defect layer.

As mentioned above, high susceptibility to external fields is an essential advantage of the CLC over other types of PCs. These fields can be used to control the helix pitch not only of the entire cholesteric, but also of part of the CLC on the left or on the right of the defect. Consider transmission spectra behavior of the structure when the CLC helix pitch is changed on the right of the defect p_2. First we analyze an initial structure of two CLC layers coupled with a dielectric defect. The transmission spectrum of the structure is shown in Fig. 3(a). There is no twist defect in this case, $\alpha = 0$, and the filling

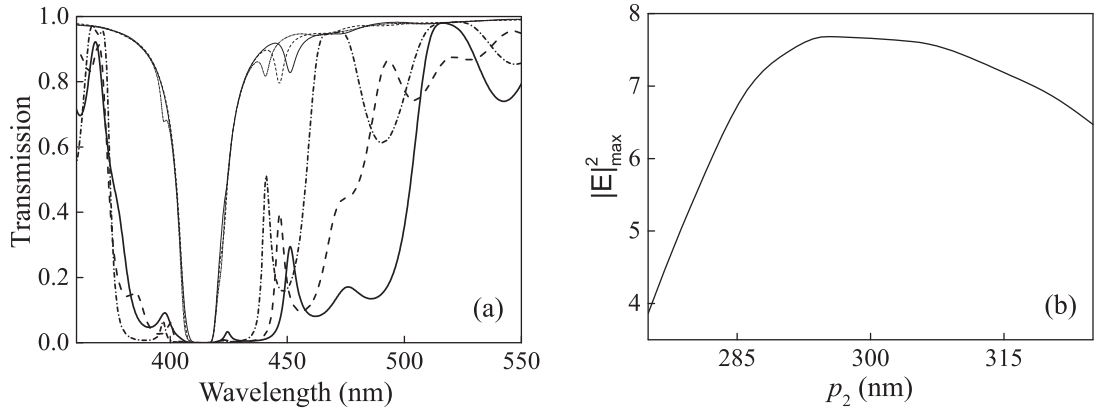

FIG. 8. (a) Transmission spectra for various p_2's, dashed-and-dotted curve: $p_2 = 275$ nm; dashed curve: $p_2 = 290$ nm; solid curve: $p_2 = 305$ nm; and $\alpha = -30°$. (b) Maximum of the squared electric field modulus of the long-wavelength defect mode as a function of the pitch p_2, $\alpha = -30°$. The bold curves refer to the right-handed circular polarizations, and the thin curves refer to the left-handed circular polarizations of light, $f = 0.02$.

factor is $f = 0$. Figure 7(a) shows the transmission spectra for two individual CLC layers with various helix pitches and for a system of these CLC layers separated by a defect.

In the figure we can see that the transmission peak occurs in the area where band gaps of the two CLCs overlap. Our calculations show that the greater the pitch of the right-side helix, the broader the PBG of the system. This fact of PBG broadening and the occurrence of a defect mode in the region of the overlapping of two scalar PCs was used to obtain a tunable asymmetric filter in a recent experiment [36].

The defect mode is shifted to the long-wavelength range of the spectrum as the right-side helix pitch grows, which results in a lower transmission coefficient in the maximum of the defect mode band. When p_2 is not sufficient for the band gaps of the two CLCs to overlap, there is no defect mode realized. Note also the nonmonotonous behavior of the squared modulus maximum of the electric field in a localized defect mode observed as the pitch p_2 grows [Fig. 7(b)]. Figure 8 illustrates the behavior of the transmission spectrum and squared field modulus of a long-wavelength defect mode for various pitches p_2 when $\alpha = -30^\circ$, $f = 0.02$, with other parameters of the system being the same. Broadening of the PBG width is observed as the pitch p_2 grows [Fig. 8(a)]. Moreover, the maximum of the squared field modulus localized in the defect mode is shifted due to the twist defect [Fig. 8(b)].

IV. CONCLUSION

We have studied spectral properties of a cholesteric liquid crystal with a resonant absorbing defect layer of a NC in the PC structure combined with a phase jump of the cholesteric helix at the interface between nanocomposite and cholesteric layers. The NC consists of silver nanoballs dispersed in a transparent glass matrix. Numerical analysis of the spectral properties and field distribution in the sample with the described structure has been carried out using the Berreman transfer matrix method. A number of important spectral features of the cholesteric with a structural defect have been revealed attributed primarily to the resonant nature of the NC effective permittivity and its essential dependence on the filling factor f.

We have studied the manifestation of the effect of splitting of defect modes induced for incident light in the transmission spectra. Frequency splitting results in a spectral band gap in the transmission spectrum. The splitting area grows with the volume fraction of nanoballs in the defect layer and can be as large as 50 nm.

We have shown that it is possible to effectively control the transmission spectrum of the CLC with a combined defect by varying the angle of incidence of light on the CLC or by applying external fields to vary the helix pitch. There are such angles of incidence or helix pitches that the NC resonant frequency appears to be close to the boundary of the band gap of a CLC structure, which facilitates the emergence of an extra transmission band for waves of both circular polarizations of incidence light.

Varying the magnitude of the phase jump of the CLC helix is a nontrivial means of control available only for chiral PCs. The transmission spectrum of the structure under study can be effectively controlled by manipulating the direction and magnitude of the twist defect.

New spectral features arise when the CLC helix pitch is modified on just one side from the defect layer. Increasing the helix pitch leads to widening of the PBG of the structure and repositioning of the defect modes. It has been revealed that the electric field maximum of the localized mode varies nonmonotonously with the helix pitch p_2.

The undertaken research is important for practical applications as it provides a further means to control the transmission spectrum and the degree of field localization in defect modes in the CLC with a combined defect as well as improves the application potential of such structures for the fabrication of novel optical devices.

ACKNOWLEDGMENTS

This work was partially supported by Grants No. 43, No. 101, and No. 24.29 of SB RAS; Russian Fund of Fundamental Research Grant No. 14-02-31248; Russian Ministry of Education and Science under the Government program, Project No. 3.1276.2014/K; Grant of the President of the Russian Federation Grant No. MK-250.2013.2, and the NSCT-SB RAS joint project.

[1] J. D. Joannopoulos, S. G. Johnson, J. N. Winn, and R. D. Meade, *Photonic Crystals: Molding the Flow of Light*, 2nd ed. (Princeton University Press, Princeton, NJ, 2008).

[2] K. Sakoda, *Optical Properties of Photonic Crystals* (Springer, Berlin, 2004).

[3] K. Busch, S. Lölkes, R. B. Wehrspohn, and H. Föll, *Photonic Crystals: Advances in Design, Fabrication, and Characterization* (Wiley-VCH, Weinheim, 2004).

[4] V. F. Shabanov, S. Ya. Vetrov, and A. V. Shabanov, *Optics of Real Photonic Crystals: Liquid Crystal Defects, Irregularities* (SB RAS, Novosibirsk, 2005) (in Russian).

[5] V. A. Belyakov, *Diffraction Optics of Complex Structured Periodic Media* (Springer-Verlag, New York, 1992).

[6] L. M. Blinov, *Structure and Properties of Liquid Crystals* (Springer, Dordrecht, 2011).

[7] I. J. Hodgkinson, Q. h. Wu, L. De Silva, M. Arnold, M. W. McCall, and A. Lakhtakia, Phys. Rev. Lett. **91**, 223903 (2003).

[8] J. Hwang, M.-H. Song, B. Park, S. Nishimura, T. Toyooka, J. W. Wu, Y. Takanishi, K. Ishikawa, and H. Takezoe, Nature Mater. **4**, 383 (2005).

[9] A. Safrani and I. Abdulhalim, Opt. Lett. **34**, 1801 (2009).

[10] A. H. Gevorgyan, M. Z. Harutyunyan, K. B. Oganesyan, and M. S. Rafayelyan, Optik **123**, 2076 (2012).

[11] H. Coles and S. Morris, Nat. Photonics **4**, 676 (2010).

[12] I. P. Il'chishin, E. A. Tikhonov, V. G. Tishchenko, and M. T. Shpak, JETP Lett. **32**, 24 (1980).

[13] S. M. Jeong, N. Y. Ha, Y. Takanishi, K. Ishikawa, H. Takezoe, S. Nishimura, and G. Suzaki, Appl. Phys. Lett. **90**, 261108 (2007).
[14] Y.-C. Yang, C.-S. Kee, J.-E. Kim, H. Y. Park, J.-C. Lee, and Y.-J. Jeon, Phys. Rev. E **60**, 6852 (1999).
[15] A. H. Gevorgyan and M. Z. Harutyunyan, Phys. Rev. E **76**, 031701 (2007).
[16] I. J. Hodkinson, Q. H. Wu, K. E. Thorn, A. Lakhtakia, and M. W. McCall, Opt. Commun. **184**, 57 (2000).
[17] V. I. Kopp and A. Z. Genack, Phys. Rev. Lett. **89**, 033901 (2002).
[18] J. Schmidtke, W. Stille, and H. Finkelmann, Phys. Rev. Lett. **90**, 083902 (2003).
[19] A. V. Shabanov, S. Ya. Vetrov, and A. Y. Karneev, JETP Lett. **80**, 181 (2004).
[20] T. Matsui, M. Ozaki, and K. Yoshino, Phys. Rev. E **69**, 061715 (2004).
[21] Y.-C. Hsiao, H.-T. Wang, and W. Lee, Opt. Express **22**, 3593 (2014).
[22] V. A. Belyakov and S. V. Semenov, J. Exp. Theor. Phys. **112**, 694 (2011).
[23] M. Becchi, S. Ponti, J. A. Reyes, and C. Oldano, Phys. Rev. B **70**, 033103 (2004).
[24] F. Wang and A. Lakhtakia, Opt. Commun. **215**, 79 (2003).
[25] J. Schmidtke and W. Stille, Eur. Phys. J. E **12**, 553 (2003).
[26] A. N. Oraevskii and I. E. Protsenko, JETP Lett. **72**, 445 (2000).
[27] S. G. Moiseev, Opt. Spectrosc. **111**, 233 (2011).
[28] E. Pedrueza, J. L. Valdes, V. Chirvony, R. Abargues, J. Hernandez-Saz, M. Herrera, S. I. Molina, and J. P. Martınez-Pastor, Adv. Funct. Mater. **21** 3502 (2011).
[29] S. Ya. Vetrov, A. Yu. Avdeeva, and I. V. Timofeev, J. Exp. Theor. Phys. **113**, 755 (2011).
[30] S. G. Moiseev, V. A. Ostatochnikov, and D. I. Sementsov, Kvantovaya Elektron. **42**, 557 (2012).
[31] S. Ya. Vetrov, M. V. Pyatnov, and I. V. Timofeev, Phys. Solid State **55**, 1697 (2013).
[32] L. A. Golovan, V. Y. Timoshenko, and P. K. Kashkarov, Phys.-Usp. **50**, 595 (2007).
[33] D. W. Berreman, J. Opt. Soc. Am. **62**, 502 (1972).
[34] S. P. Palto, J. Exp. Theor. Phys. **92**, 552 (2001).
[35] I. V. Timofeev, Y.-T. Lin, V. A. Gunyakov, S. A. Myslivets, V. G. Arkhipkin, S. Ya. Vetrov, W. Lee, and V. Y. Zyryanov, Phys. Rev. E **85**, 011705 (2012).
[36] H.-T. Wang, I. V. Timofeev, K. Chang, V. Y. Zyryanov, and W. Lee, Opt. Express **22**, 15097 (2014).